

2.27 ANGLE TRACKING

For a radar to maintain optimum track on a moving target, it must continually adjust its antenna position so that it remains pointing at the target. The primary output of most radar tracking systems is the target location determined by the pointing angles of the antenna beam and the positions of the range tracking gates. In missile guidance applications, accurate angle measurement precision and future prediction at high sampling rates are generally required (see Reference m, pages 18.1-18.3). Angle tracking systems extract and process target off-boresight error measurements to reposition antenna pointing servos in an attempt to maintain small error measurements. This closed-loop process forms the basis for the angle track functional element.

Although there are several angle tracking methods available, this functional element will focus on two main types of monopulse tracking radars (see Reference m, pages 18.8-18.17). These two types are referred to as two-channel and three-channel monopulse systems. In the three-channel monopulse system, the azimuth and elevation channels remain isolated throughout the process. In the two-channel system, the azimuth and elevation channels are combined at the beginning of the process and individual responses are extracted at the end of the process. In general, monopulse radars operate on a simultaneous lobing principle where the antenna response is split into four lobes corresponding to the four angle tracking quadrants. Signal returns from the four quadrants are simultaneously added and subtracted to generate off-boresight error measurements. These measurements take the form of an elevation difference signal formed by subtracting the upper quadrant returns from the lower quadrant returns, an azimuth difference signal formed by subtracting left quadrant returns from right quadrant returns, and a sum signal formed by adding together all four quadrant returns.

2.27.1 Functional Element Design Requirements

This section contains the design requirements necessary to implement the simulation of angle tracking in ESAMS 2.6.2.

1. ESAMS will generate azimuth and elevation tracking errors computed from antenna sum and difference signals generated by the antenna gain functional element will be used as input to the angle tracking element. These signals will be processed to produce off-boresight azimuth and elevation errors that will in turn be used as input to the antenna pointing servo algorithm.
2. ESAMS will compute tracking error angles using the appropriate monopulse methodology for both azimuth and elevation.
3. ESAMS will simulate the response of the antenna pedestal drive system to the computed azimuth and elevation error angles.

2.27.2 Functional Element Design Approach

This section describes the design elements that implement angle track design requirements. A design element is an algorithm or feature that represents a specific component of the functional element (FE) design.

A three-channel monopulse system maintains three separate signal channels for processing the sum and difference signals. The block diagram in Figure 2.27-1 shows the signal flow

of a three-channel system. To maintain a stable closed-loop track, signal amplitude fluctuations that do not depend on off-boresight position must be removed by normalization. The output of the normalization stage is the ratio of the difference channel signals to the sum channel signal. Normalization is accomplished using either a logarithmic amplifier or an Automatic Gain Control (AGC) filter. The demodulation stage forms the azimuth and elevation off-boresight error angles which are directly proportional to the normalized difference channel signals.

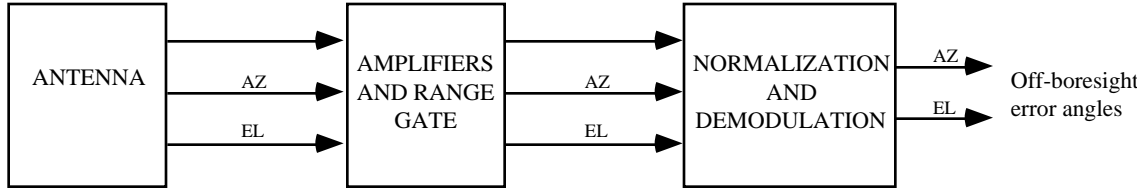


FIGURE 2.27-1. Three-Channel Monopulse Block Diagram.

A two-channel system combines the azimuth and elevation difference signals into a single channel using a microwave resolver and are later demodulated to form the off-boresight error angles using the resolver as a reference. The two-channel operation is shown in Figure 2.27-2.

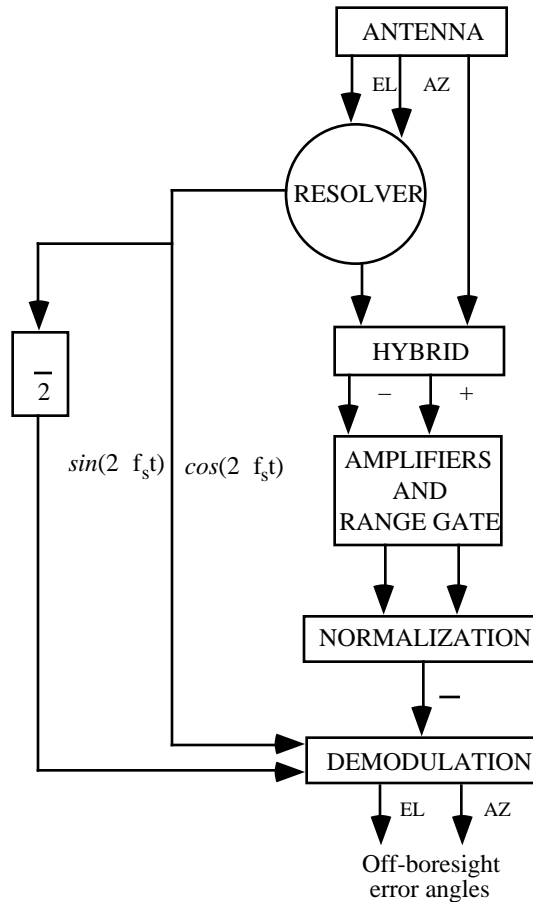


FIGURE 2.27-2. Two-Channel Monopulse Block Diagram.

The angle track functional element in ESAMS will consist of two- and three-channel monopulse implementations similar to those shown in Figures 2.27-1 and 2.27-2. The functional element is intended to compute azimuth and elevation errors generated by these tracking systems in order to account for the effects of the methodologies on the performance of angle tracking.

Design Element 27-1: Two-channel Resolver

The purpose of the two-channel resolver is to combine the azimuth and elevation difference channel signals into a single quadrature signal for a two-channel system. The resolver itself is a mechanical device that consists of a coupling loop rotated in a circular waveguide at a fixed angular frequency $2 f_s$. The azimuth difference channel signal AZ , and elevation difference signal EL , are coupled by the resolver to form (see Reference m, pages 18.20-18.21).

$$i = AZ_i \cos(2 f_s t) + EL_i \sin(2 f_s t) \quad [27.7-1]$$

where the subscript i denotes each signal component generated by the antenna response modules. The cosine term is referred to as the in-phase (I) component and the sine term is referred to as the quadrature (Q) component. The output of the resolver is combined at the hybrid stage with the sum channel signals S_i , to form the main signal channel

$$AZ_i = i + i \quad [2.27-2]$$

and the auxiliary signal channel

$$EL_i = i - i \quad [2.27-3]$$

Design Element 27-2: Two-channel Range Gate and Normalization

In the two-channel system, the main and auxiliary signals are passed through range gates to eliminate unwanted target returns and reduce noise. This effect is captured by multiplying the main and auxiliary channels by a factor representing the fraction of the return pulse visible in the range gate for each signal component. The gated signals are then summed to form composite main and auxiliary channel signals:

$$\begin{aligned} + &= \sum_{i=1}^N i [i + i] \\ - &= \sum_{i=1}^N i [i - i] \end{aligned} \quad [2.27-4]$$

where i = the fraction of the i^{th} signal component pulse visible in the range gate
 N = the total number of signal components generated by the antenna response modules

The normalization stage in monopulse systems usually involves a logarithmic amplifier or AGC filter. The effect of this stage is to normalize, or divide the quadrature signal D by the

sum channel signal. Log amplifiers and AGC filters approximate this ratio. Logarithmic amplification will tend to provide an instantaneous AGC response, whereas AGC filtering will impose a phase delay on the signal output. The two-channel monopulse implementation will assume an instantaneous normalization process whose output can be represented by the ratio

$$N = \frac{\begin{vmatrix} + & - \\ + & - \end{vmatrix}}{\begin{vmatrix} + & + \\ - & - \end{vmatrix}} = - \quad [2.27-5]$$

The right-hand-side equality in the above equation is valid as long as N , which is generally true during target track.

Design Element 27-3: Two-channel Angle Demodulator

To compute the off-boresight error angles AZ and EL for the two-channel system, the angle demodulator extracts the in-phase and quadrature components from the normalized error signal N . These components are extracted by forming the inner products:

$$\begin{aligned} A &= 2f_s \int_0^s N \cos(2f_s t) dt \\ &= 2f_s \int_0^s \frac{1}{2} \cos(2f_s t) [AZ \cos(2f_s t) + EL \sin(2f_s t)] dt \\ E &= 2f_s \int_0^s N \sin(2f_s t) dt \\ &= 2f_s \int_0^s \frac{1}{2} \sin(2f_s t) [AZ \cos(2f_s t) + EL \sin(2f_s t)] dt \end{aligned} \quad [2.27-6]$$

where s = resolver scan period ($s = 1/f_s$)

Note that the azimuth and elevation difference values AZ and EL , in Equations [2.27-6] are composite values, that is

$$AZ = \frac{1}{N} \sum_{i=1}^N AZ_i, \quad EL = \frac{1}{N} \sum_{i=1}^N EL_i \quad [2.27-7]$$

Performing the integration in Equations [2.27-6] under the assumption that the sum and difference values change slowly relative to the scan frequency gives

$$\begin{aligned} A &= \frac{AZ}{2} \\ E &= \frac{EL}{2} \end{aligned} \quad [2.27-8]$$

The two-channel demodulator will operate on a discrete time-step, hence the continuous-time inner products in Equations [2.27-6] must be transformed to the discrete-time equivalent:

$$\begin{aligned} A &= \frac{AZ}{M} = 2 \sum_{n=0}^{M-1} \frac{f_s}{M} \cos \frac{2\pi n}{M} \left(AZ \cos \frac{2\pi n}{M} + EL \sin \frac{2\pi n}{M} \right) T \\ E &= \frac{EL}{M} = 2 \sum_{n=0}^{M-1} \frac{f_s}{M} \sin \frac{2\pi n}{M} \left(AZ \cos \frac{2\pi n}{M} + EL \sin \frac{2\pi n}{M} \right) T \end{aligned} \quad [2.27-9]$$

where M = the number of samples within a scan period
 T = sampling time-step

Design Element 27-4: Two-channel Error Angle

The error angle characteristics of the antenna must be known to relate the demodulated azimuth and elevation signals to off-boresight error angles. If the off-boresight error angles are small, then the antenna difference patterns can be approximated by sine functions, and the sum channel antenna pattern can be approximated by a cosine function (see Antenna Gain FE in Section 2.20):

$$\begin{aligned} A &= \frac{AZ}{M} \frac{V \sin(K_1 AZ)}{V \cos(K_1 AZ)} K_1 AZ \\ E &= \frac{EL}{M} \frac{V \sin(K_2 EL)}{V \cos(K_2 EL)} K_2 EL \end{aligned} \quad [2.27-10]$$

where K_1 and K_2 = azimuth and elevation antenna error slopes
 V = antenna voltage

Now, the off-boresight error angles are given as

$$\begin{aligned} AZ &= \frac{1}{K_1} \frac{AZ}{M} \\ EL &= \frac{1}{K_2} \frac{EL}{M} \end{aligned} \quad [2.27-11]$$

Summing equation [2.27-9] and combining it with equation [2.27-11] allows for the solution of the off-boresight angles.

The output of Algorithm 2.27-1 at each time step are the off-boresight angle errors AZ and EL . Initially, the stack will not be completely filled until M steps of the algorithm have been executed. As a result the off-boresight error angles will be set to zero during the first $M-1$ sampling periods.

Design Element 27-5: Antenna Pedestal Dynamics

The final stage of the angle tracking process for both the two- and three-channel systems accounts for the positioning dynamics of the antenna pedestal. Antenna positioning servos will be modeled as a closed-loop controller whose configuration is shown in Figure 2.27-3.

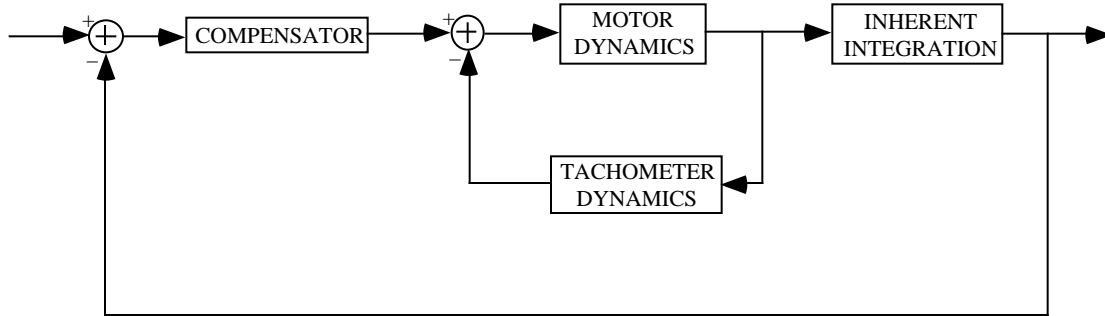


FIGURE 2.27-3. Antenna Positioning Servo Configuration.

The inner loop of the double loop configuration shown in Figure 2.27-3 represents the antenna pedestal positioning motor and feed-back control. The outer portion of the loop provides dynamic compensation and a low-pass representation of the mechanical pedestal. If the inner loop is considered to be very fast relative to the outer loop, then it can be collapsed to a constant gain value. The resulting control loop shown in Figure 2.27-4 is referred to as an “improved type I” servo.

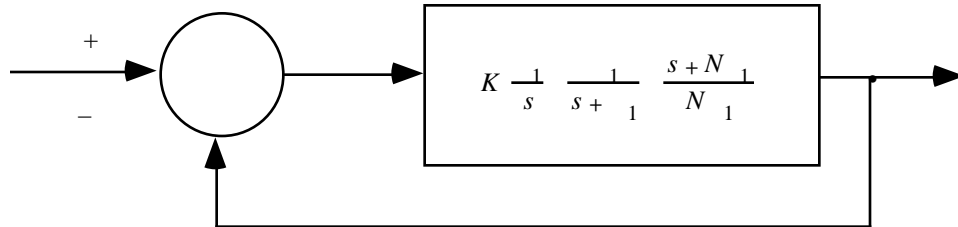


FIGURE 2.27-4. Improved Type I Servo.

The open-loop transfer function $T(s)$ from Figure 2.27-4 is (see Reference n, pages 250-253)

$$T(s) = K \frac{1}{s} \frac{1}{s + 1} \frac{s + N}{N} \quad [2.27-12]$$

where N and K represent ratios of characteristic break frequencies. The configuration in Figure 2.27-4 leads to the closed-loop transfer function

$$H(s) = \frac{T(s)}{1 + T(s)} = \frac{s + N}{N} \frac{K}{s^2 + \frac{1}{N}(N + K)s + K} \quad [2.27-13]$$

If the following substitutions are made:

$$\begin{aligned} &= N - 1 \\ 2 &= \frac{1}{N} (N + K) \\ 2 + 2 &= K - 1 \end{aligned} \quad [2.27-14]$$

then $H(s)$ can be written as

$$H(s) = \frac{2 + 2}{s^2 + 2s + \left(2 + 2\right)} \frac{(s +)}{(s +)} \quad [2.27-15]$$

where

$$= 1 \sqrt{K - \frac{1}{4N} (N + K)^2} \quad [2.27-16]$$

Now the time response of the antenna position servos is given by the solution of the differential equation

$$\ddot{y}(t) + 2 \dot{y}(t) + \left(2 + 2\right)y(t) = \frac{2 + 2}{(s +)} (\dot{x}(t) + x(t)) \quad [2.27-17]$$

where $x(t)$ denotes the continuous-time input signal, and $y(t)$ denotes the continuous output response. Since the antenna position servos will be updated on a discrete time interval T , this differential equation must be transformed into a discrete-time difference equation. This is accomplished using step-invariant pole-matching.

The step-invariant pole matching method maps a transfer function from Laplace space into Z-space while preserving the system response to a step input. This mapping can be expressed as

$$H(s) \rightarrow \bar{H}(z) = kG(z) \quad [2.27-18]$$

where $\bar{H}(z)$ is the Z-space transfer function, $G(z)$ is a polynomial in z formed by pole and zero substitution, and k is a constant.

The closed-loop transfer function in Equation [2.27-15] has a zero at $s_{zero} = -$, and a conjugate pair of poles at $s_{pole1} = - + j$ and $s_{pole2} = - - j$. Pole matching requires that the poles and zeros of the Laplace space transfer function be mapped into the poles and zeros of the Z-space transfer function according to the relationships

$$\begin{aligned} z_{pole} &= e^{s_{pole} T} \\ z_{zero} &= e^{s_{zero} T} \end{aligned} \quad [2.27-19]$$

This mapping yields

$$z_{pole1} = e^{(- + j) T}$$

$$\begin{aligned} z_{pole2} &= e^{(-j)T} \\ z_{zero} &= e^{-T} \end{aligned} \quad [2.27-20]$$

Substituting these poles and zeros into the Laplace-space transfer function gives the Z-space transfer function:

$$G(z) = \frac{z^2 + 2}{z - e^{(-j)T}} \frac{z - e^{(-T)}}{z - e^{(-j)T}} \quad [2.27-21]$$

Next, the final values of the continuous and discrete time step responses are matched:

$$\begin{aligned} 1 &= \lim_{s \rightarrow 0} sH(s) \frac{1}{s} = \lim_{z \rightarrow 1} \frac{z-1}{z} kG(z) \frac{z}{z-1} = \\ &k \frac{z^2 + 2}{1 - e^{(-j)T}} \frac{(1 - e^{-T})}{1 - e^{(-j)T}} \end{aligned} \quad [2.27-22]$$

so that

$$k = \frac{1 - e^{(-j)T}}{2 + 2} \frac{1 - e^{(-T)}}{(1 - e^{(-j)T})} \quad [2.27-23]$$

Now, the Z-space transfer function can be written as

$$\bar{H}(z) = kG(z) = \frac{(1 - 2e^{-T} \cos(T) + e^{-2T})(1 - e^{-T}z^{-1})}{(1 - 2e^{-T} \cos(T)z^{-1} + e^{-2T}z^{-2})} \quad [2.27-24]$$

and the difference equation for the antenna position servo response is given by

$$\begin{aligned} y(t) &= 2e^{-T} \cos(T)y(t-T) - e^{-2T}y(t-2T) + \\ &\frac{(1 - 2e^{-T} \cos(T) + e^{-2T})}{(1 - e^{-T})} [x(t) - e^{-T}x(t-T)] \end{aligned} \quad [2.27-25]$$

This difference equation, which is used for both azimuth and elevation channels, can be written in simpler form as

$$y(t) = c_1y(t-T) + c_2y(t-2T) + c_3x(t) + c_4x(t-T) \quad [2.27-26]$$

where the constants are defined

$$\begin{aligned} c_1 &= 2e^{-T} \cos\left(\frac{T}{2}\right) \\ c_2 &= -e^{-2T} \\ c_3 &= \frac{1 - 2e^{-T} \cos\left(\frac{T}{2}\right) + e^{-2T}}{1 - e^{-T}} \\ c_4 &= -c_3 e^{-T} \end{aligned} \quad [2.27-27]$$

Azimuth and elevation tracking rates are computed by considering the rate transfer function $H(s) = sH(s)$. This transfer function will have poles at $s_{pole1} = -\frac{1}{T} + j$ and $s_{pole2} = -\frac{1}{T} - j$, and zeros at $s_{zero1} = 0$ and $s_{zero2} = -\frac{1}{T}$. In this case a ramp invariant pole matching procedure is used to generate the Z-space rate transfer function:

$$\bar{H}(z) = \frac{(1 - 2e^{-T} \cos\left(\frac{T}{2}\right) + e^{-2T})(1 - z^{-1})(1 - e^{-T} z^{-1})}{T(1 - e^{-T})(1 - 2e^{-T} \cos\left(\frac{T}{2}\right)z^{-1} + e^{-2T} z^{-2})} \quad [2.27-28]$$

which yields the rate difference equation

$$\begin{aligned} \dot{y}(t) &= 2e^{-T} \cos\left(\frac{T}{2}\right) \dot{y}(t-T) - e^{-2T} \dot{y}(t-2T) + \\ &\quad \frac{(1 - 2e^{-T} \cos\left(\frac{T}{2}\right) + e^{-2T})}{T(1 - e^{-T})} x(t) - \\ &\quad \frac{(1 + e^{-T})(1 - 2e^{-T} \cos\left(\frac{T}{2}\right) + e^{-2T})}{T(1 - e^{-T})} x(t-T) + \\ &\quad \frac{e^{-T}(1 - 2e^{-T} \cos\left(\frac{T}{2}\right) + e^{-2T})}{T(1 - e^{-T})} x(t-2T) \end{aligned} \quad [2.27-29]$$

This difference equation can be expressed as

$$\dot{y}(t) = c_1 \dot{y}(t-T) + c_2 \dot{y}(t-2T) + c_3 x(t) + c_4 x(t-T) + c_5 x(t-2T) \quad [2.27-30]$$

where the constants are defined by

$$\begin{aligned} c_1 &= 2e^{-T} \cos\left(\frac{T}{2}\right) \\ c_2 &= -e^{-2T} \\ c_3 &= \frac{1 - c_1 - c_2}{T(1 - e^{-T})} \\ c_4 &= \frac{-(1 - c_1 - c_2)(1 + e^{-T})}{T(1 - e^{-T})} \\ c_5 &= \frac{(1 - c_1 - c_2)e^{-T}}{T(1 - e^{-T})} \end{aligned} \quad [2.27-31]$$

The inputs to the antenna position and rate servo difference equations must be given in the inertial frame of reference whereas the off-boresight error angles are measured in the boresight frame of reference. Since the inertial and boresight reference frame centers coincide, the transformation is accomplished by projecting the off-boresight azimuth error angle onto the horizontal plane of the inertial frame:

$$AZ = AZ + \frac{AZ}{\cos(EL)} \quad [2.27-32]$$

where AZ and EL =boresight azimuth and elevation angles in the inertial reference frame.

Design Element 27-6: Three-channel Composite Signals

For three-channel monopulse system, the sum and two difference channel signal components generated by the antenna response modules are multiplied by a range gate attenuation factor that represents the fraction of the signal that is visible within the range gate. The signal components are then summed to produce the composite signals of the sum channel , azimuth difference channel AZ and elevation difference channel EL :

$$\begin{aligned} &= \sum_{i=1}^N i \quad i \\ &AZ = \sum_{i=1}^N i \quad AZ_i \\ &EL = \sum_{i=1}^N i \quad EL_i \end{aligned} \quad [2.27-33]$$

where i = the fraction of the i^{th} signal component pulse visible in the range gate
 N = the total number of signal components generated by the antenna response modules

Design Element 27-7: Three-channel Normalization

The azimuth and elevation channel signals must be normalized to maintain stability. Since the normalization step performs a division of the difference channel signals by the sum channel, precautions must be taken to ensure that a division by a small number does not take place. This is accomplished by examining the magnitude of the sum channel signal. If the magnitude exceeds a preset level , then the signal ratios are formed directly:

$$\begin{aligned} A &= \frac{AZ}{\text{sum}} \\ E &= \frac{EL}{\text{sum}} \end{aligned} \quad [2.27-34]$$

If the sum channel magnitude does not exceed ϵ , but is not zero, then the magnitude of the sum channel signal is set to ϵ and the ratios are formed:

[Note to developer: why ϵ ?]

$$\begin{aligned} \overline{| |} &= e^j \\ A &= \frac{AZ}{\epsilon e^j} \\ E &= \frac{EL}{\epsilon e^j} \end{aligned} \quad [2.27-35]$$

If the sum channel signal is identically zero then the sum channel phase can not be extracted and a random phase must be computed. This is accomplished by drawing a uniform random phase angle θ , from the interval $[0, 2\pi]$, and then forming the sum channel signal

$$= \epsilon (\cos(\theta) + j \sin(\theta)) \quad [2.27-36]$$

The azimuth and elevation ratios are formed as in Equation [2.27-35].

Design Element 27-8: Three-channel Error Angles

As in design element 27-4, the error angle characteristics represented by the antenna error slopes are used to relate the normalized azimuth and elevation signals to off-boresight error angles. In the three-channel case, the normalized azimuth and elevation channels are complex numbers. The off-boresight error angles are computed using the antenna error slopes and the real portion of the normalized channel signals according to:

$$\begin{aligned} AZ &= \frac{1}{K_1} \text{Re}(A) \\ EL &= \frac{1}{K_2} \text{Re}(E) \end{aligned} \quad [2.27-37]$$

where K_1 and K_2 = azimuth and elevation antenna error slopes

2.27.3 Functional Element Software Design

This section contains the software design necessary to implement the functional element requirement described in Section 2.27.1 and the design approach described in Section 2.27.2. It is organized as follows: the first part describes the subroutine hierarchy and gives descriptions of the relevant subroutines; the next part contains logical flow charts and describes important operations represented by each block in the charts; the last part contains a description of all input and output data for the FE as a whole and for each subroutine that implements the Angle Track FE.

The FORTRAN call tree implemented for the Angle Track FE in the ESAMS 2.6.2 code is shown in Figure 2.27-5. The diagram depicts the structure of the entire model for this FE,

from ZINGER (the main program) through the least significant subroutine implementing this FE. Subroutines which directly implement the FE appear as shaded blocks. Each of these subroutines is briefly described in Table 27-6.

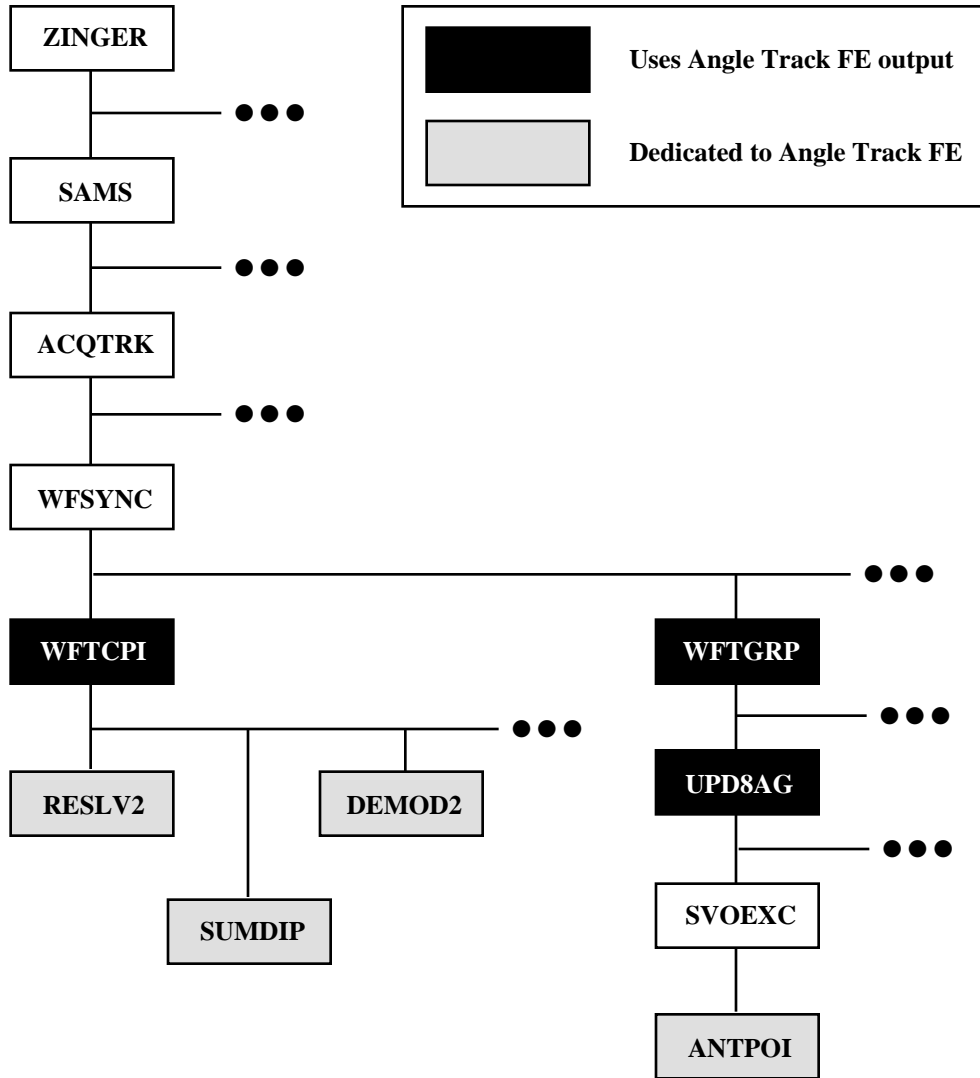


FIGURE 2.27-5. Call Hierarchy for Angle Track.

TABLE 2.27-1. Subroutines Descriptions.

RESLV2	Simulates the operation of the two-channel resolver. The routine receives as input, the azimuth and elevation difference channel signals computed by the antenna response modules, forms the modulated quadrature signal ϕ , and combines it with the sum channel signal to form the two-channel main and auxiliary channel signals $\phi + \psi$ and $\phi - \psi$.
DEMOD2	Simulates the operation of the two-channel monopulse demodulator. The routine receives as input the main and auxiliary channel signals and produces the azimuth and elevation off-boresight error angles at each time step.
ANTPOI	Initializes the antenna pedestal servo constants and difference equations.

TABLE 2.27-1. Subroutines Descriptions. (Contd.)

RESLV2	Simulates the operation of the two-channel resolver. The routine receives as input, the azimuth and elevation difference channel signals computed by the antenna response modules, forms the modulated quadrature signal, and combines it with the sum channel signal to form the two-channel main and auxiliary channel signals $+$ and $-$.
SVOEXC	Simulates the motion of the antenna pedestal as it is repositioned during angle track update. The routine receives as input the azimuth and elevation off-boresight error angles and updates a set of discrete-time difference equations.
SUMDIF	Combines the sum and difference channel signals, detects the phase of the difference channels with respect to the sum channel and computes the azimuth and elevation off-boresight error angles for a three-channel monopulse system.

Angle Track Logic Flow

The block diagram in Figure 2.27-6 shows the functions that determine the impact of two-channel monopulse processing on target tracking. Each block contains a specific function and the subroutine in which that function will occur. The names of the subroutines are in parentheses.

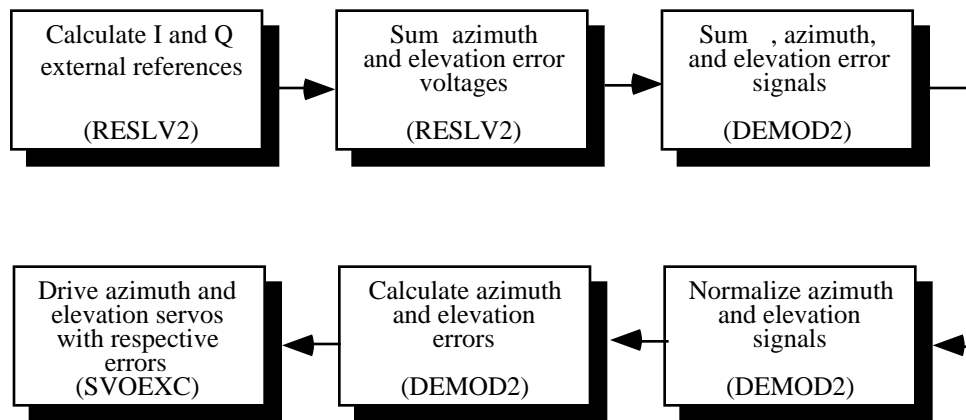


FIGURE 2.27-6. Two-Channel Angle Track Block Diagram.

The block diagram in Figure 2.27-7 shows the functions that determine the impact of the three-channel monopulse processing on target tracking. Each block contains a specific function and the subroutine in which that function will occur. The names of the subroutines are in parentheses.

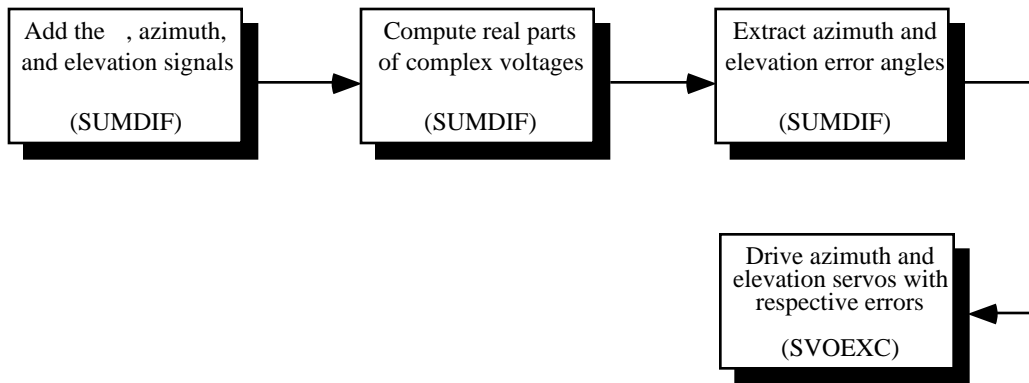


FIGURE 2.27-7. Three-Channel Angle Track Block Diagram.

Figure 2.27-8 shows the logic flow chart for subroutine RESLV2. The numbered blocks in the flow chart are discussed below.

[Note to developer: Logic involving the AGC and Log filters has been omitted since they are considered experimental and can be removed without notice.]

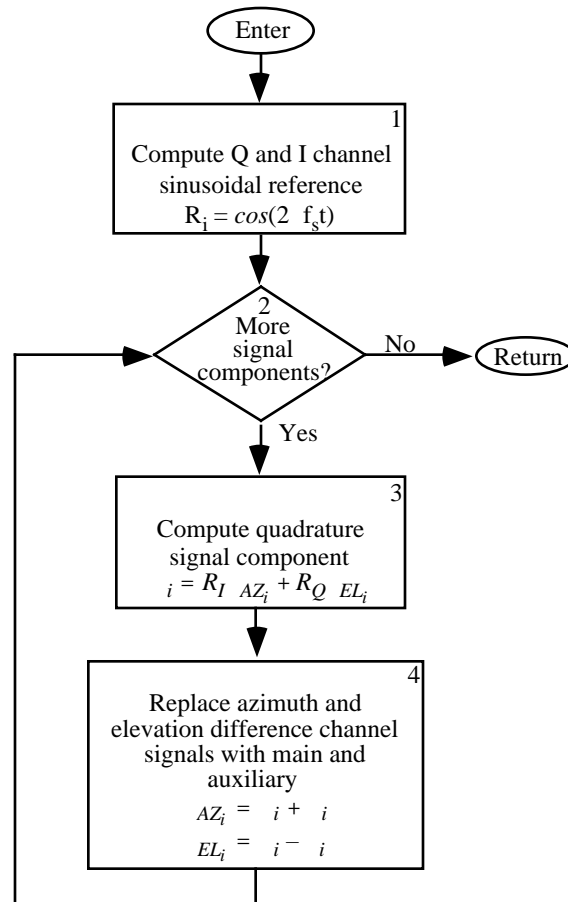


FIGURE 2.27-8. Subroutine RESLV2 Logic Flow Chart.

Block 1. The reference signal in-phase (cosine) and quadrature (sine) components are computed at the current time step.

Block 2. This step marks the beginning of a loop that will process all signal components generated by the antenna response modules through the two-channel resolver.

Block 3. The quadrature signal is computed from the reference signal components and the azimuth and elevation difference channel signals. This step implements Equation [2.27-1].

Block 4. The two-channel main and auxiliary signals are formed and replace the azimuth and elevation difference channel signals. The main and auxiliary channel signals are given by Equations [2.27-2] and [2.27-3].

Figure 2.27-9 shows the logic flow chart for subroutine DEMOD2. The numbered blocks in the flow chart are discussed below.

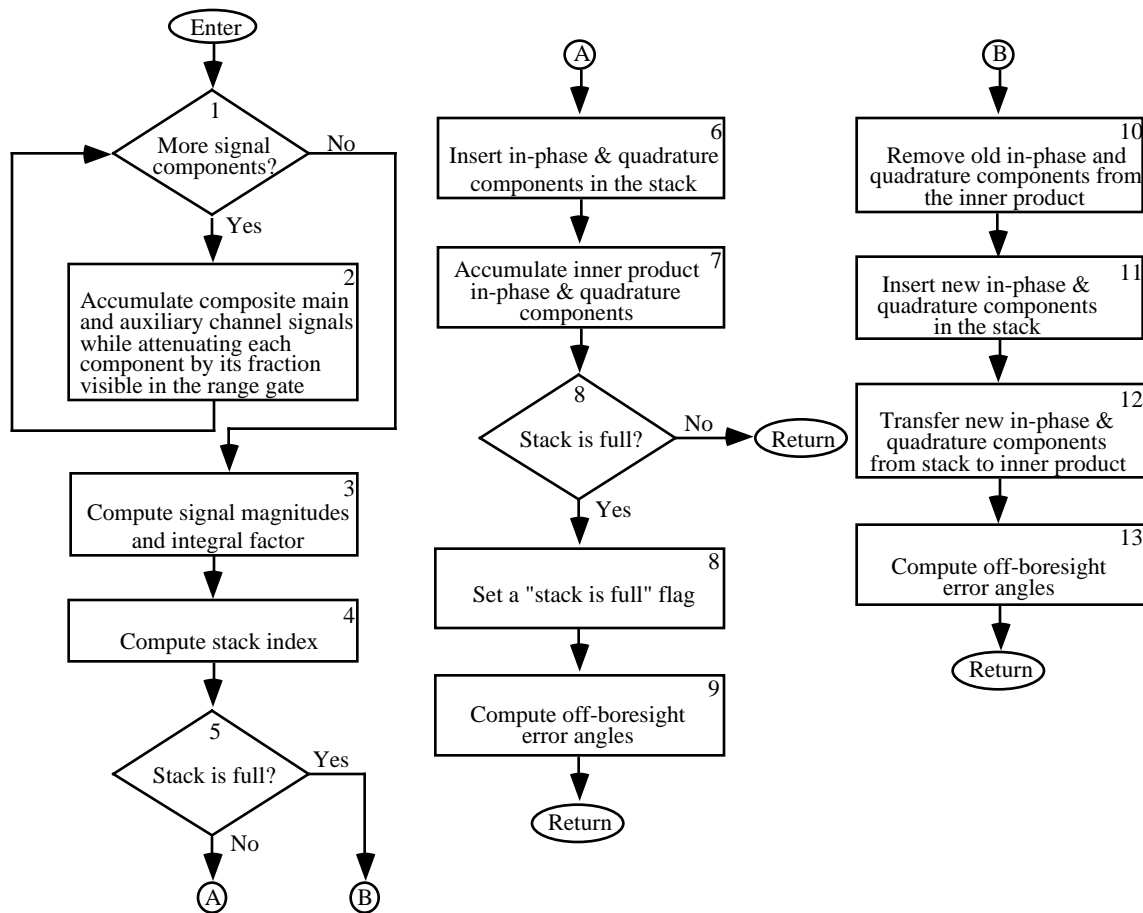


FIGURE 2.27-9. Subroutine DEMOD2 Logic Flow Chart.

Block 1. This first step marks the beginning of a loop that processes all signal components generated by the antenna response modules through a composite signal accumulator.

Block 2. This step attenuates each main and auxiliary signal component according to the fraction of that signal visible within the range gate and then adds these signals to a composite signal accumulation.

Block 3. The main and auxiliary channel signal magnitudes and integral factor are computed in preparation for inner product update. The integral factor is the product of the current resolver output signal, the resolver scan frequency and the simulation time step.

Block 4. The current index to the stack is computed at this step. The index is always between 1 and the total number of samples.

Block 5. This conditional step checks a flag (NLATCH) to determine whether or not the demodulator stack has been filled. If the flag has not been set (NLATCH=0), then the stack and inner product will be updated but the demodulator output will be held at zero.

Block 6. The product of the in-phase and quadrature components and the integral factor are inserted into the stack at the current position.

Block 7. The product of the in-phase and quadrature components and the integral factor are added to the inner product accumulator. This step represents the summing process of Equation [2.27-9].

Block 8. This conditional block determines if the stack has been filled and is ready for output. The condition is checked by comparing the stack index to the total number of samples for equality. If the condition is met, then a stack-full flag is set (NLATCH=1)

Block 9. If the conditional in Block 8 has been met, then the off-boresight error angles are computed according to Equation [2.27-11].

Block 10. The old values of the in-phase and quadrature signals at the same position of the previous scan are removed from the inner product accumulation.

Block 11. The current product of the in-phase and quadrature components and the integral factor are inserted into the stack.

Block 12. The current product of the in-phase and quadrature components and the integral factor are added to the inner product accumulator. This step represents the summing process of Equation [2.27-9].

Block 13. The off-boresight error angles are computed according to Equation [2.27-11].

Figure 2.27-10 shows the logic flow chart for subroutine ANTPOI. The numbered blocks in the flow chart are discussed below.

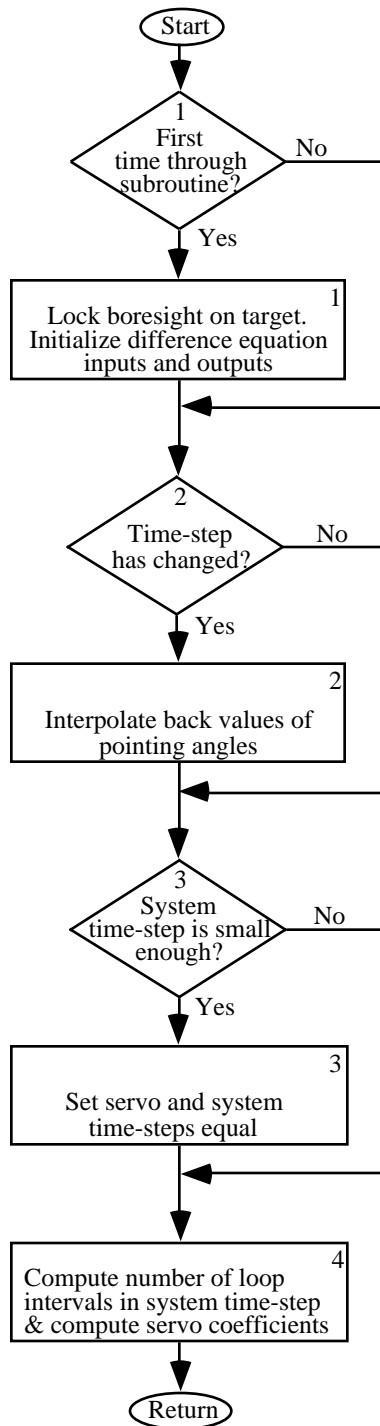


FIGURE 2.27-10. Subroutine ANTPOI Logic Flow Chart.

Block 1. The conditional first step determines whether the subroutine is being called for the first time. If so, the initial pointing angles are set to the boresight position.

Block 2. This step determines whether the subroutine has been called as the result of a change in system time-step. If so, azimuth and elevation pointing angle back values are computed by interpolation.

Block 3. This step determines whether the system time-step increment is short enough to be used as the servo time-step. If so, the servo time-step is set equal to the system time-step.

Block 4. The number of servo update intervals within a system time-step is computed and the servo constants of Equations [2.27-27] and [2.27-31] are computed.

Figure 2.27-11 shows the logic flow chart for subroutine SVOEXC. The numbered blocks in the flow chart are discussed below.

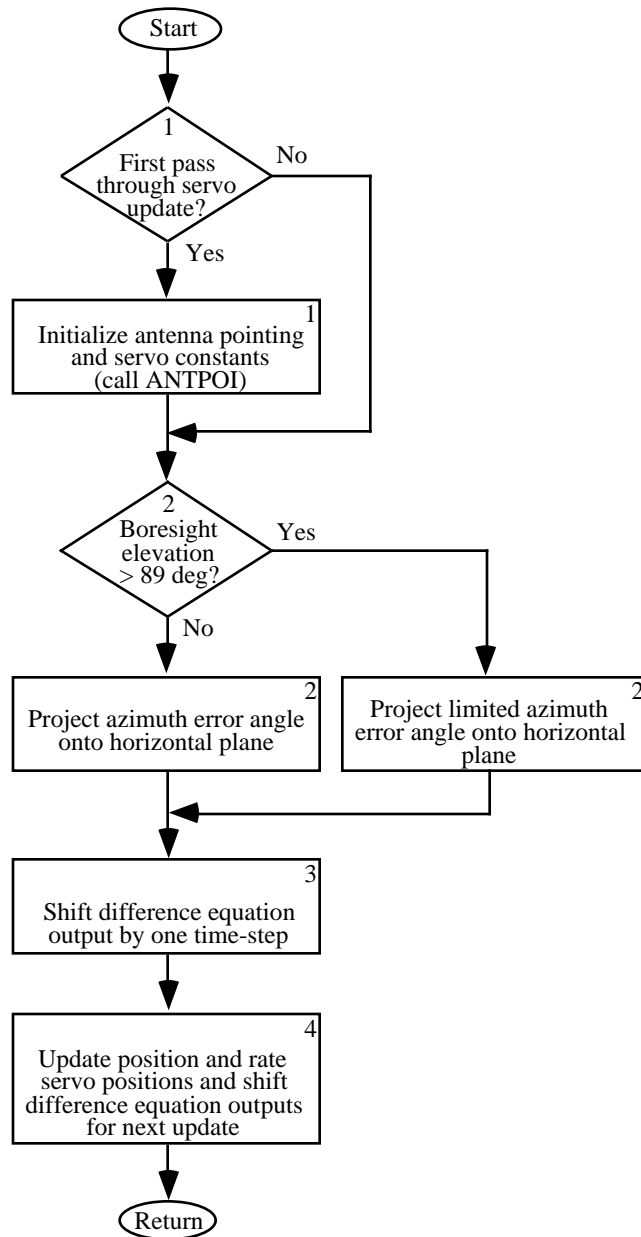


FIGURE 2.27-11. Subroutine SVOEXC Logic Flow Chart.

Block 1. This conditional step determines whether the servo equations and constants have been initialized or if the time-step has changed in which case a call is made to the servo initialization routine ANTPOI.

Block 2. This step determines whether the boresight elevation angle is greater than 89 degrees. If it is not, then the azimuth servo input is generated by projecting the azimuth error angle from the boresight frame of reference onto the horizontal plane of the inertial reference frame according to Equation [2.27-31]. If the elevation error is greater than 89 degrees then the projection is based on an elevation error angle limited to 89 degrees.

Block 3. Previous difference equation inputs and outputs are delayed by a single time-step.

Block 4. This step updates the position and rate difference equations according to Equations [2.27-26] and [2.27-30].

Figure 2.27-12 shows the logic flow chart for subroutine SUMDIF. The numbered blocks in the flow chart are discussed below.

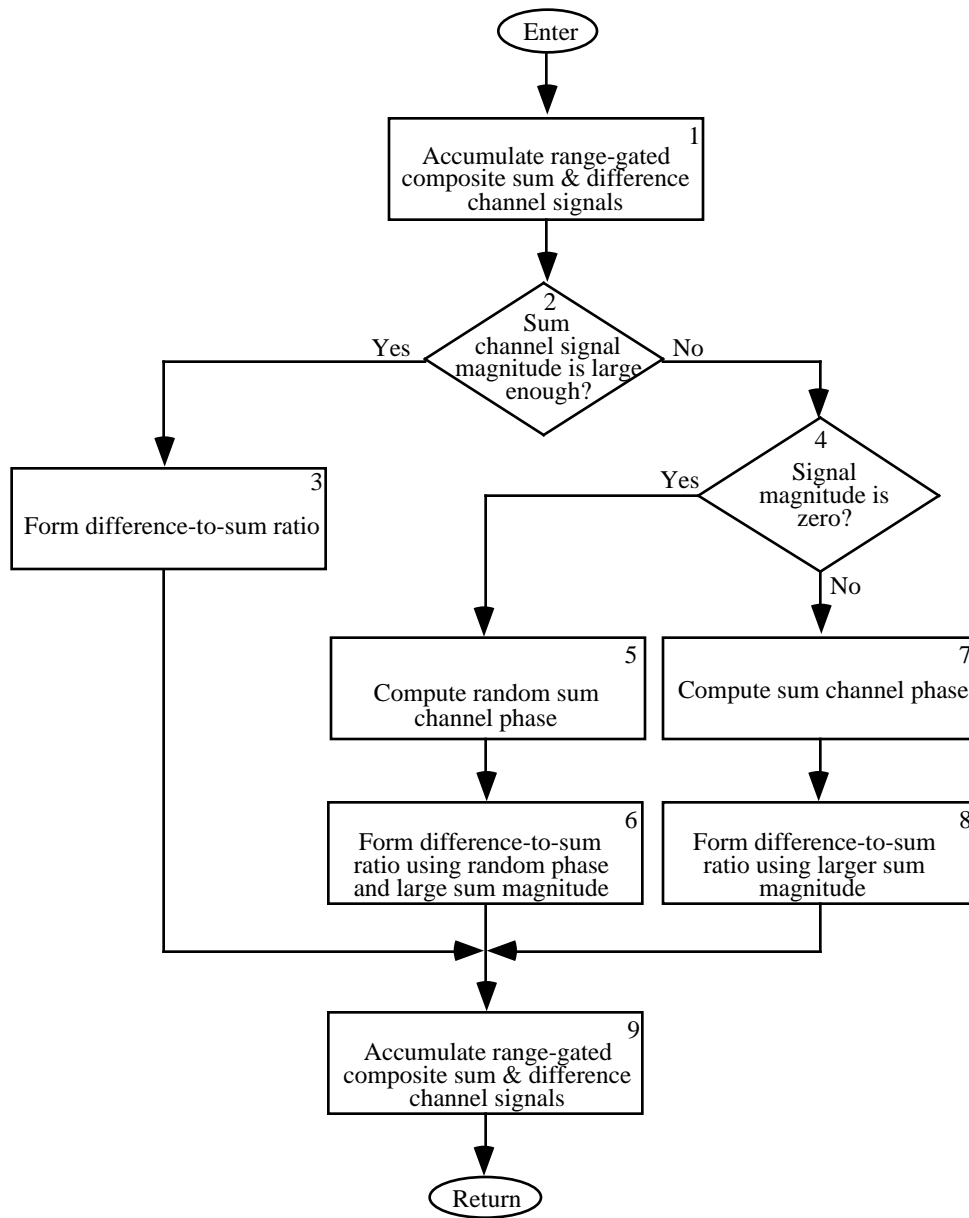


FIGURE 2.27-12. Subroutine SUMDIF Logic Flow Chart.

Block 1. Each sum and difference channel signal component generated by the antenna response modules are attenuated by the fraction of that signal pulse visible in the range gate and then added to the composite sum and difference channel signal.

Block 2. This conditional step determines whether the magnitude of the sum channel signal is larger than a preset small value (EPSILN).

Block 3. If it has been determined in Block 2 that the magnitude of the sum channel signal is large enough, then the difference-to-sum channel ratio is formed and the real part of this value is stored for error angle calculation.

Block 4. This conditional step determines whether the magnitude of the sum channel signal is identically zero.

Block 5. If it has been determined in Block 4 that the magnitude of the sum channel signal is identically zero, then a sum channel phase is determined by a uniform random draw.

Block 6. The difference-to-sum channel ratio is formed using a larger sum channel amplitude (EPSILN**5).

Block 7. If it has been determined in Block 4 that the magnitude of the sum channel signal is not identically zero, then the sum channel phase is computed.

Block 8. The difference-to-sum channel ratio is formed using a larger sum channel amplitude (EPSILN**5). This computation reflects Equation [2.27-35].

Block 9. The off-boresight error angles are computed according to Equation [2.27-37].

2.27.3.1 Angle Track Inputs and Outputs

The outputs of this FE are updated azimuth and elevation angles and rates of the radar pedestal. These are given in Table 2.27-2. In the selection of the missile/radar system to be used, several variables used in Angle Track are indirectly set by the user. These variables consist of flags which identify the system and constants which are used to compute the system-specific coefficients.

TABLE 2.27-2. Angle Track Outputs.

Variable Name	Description
BOREAZ	Updated boresight azimuth angle
AZRATE	Updated azimuth tracking rate
BOREEL	Updated boresight elevation angle
ELRATE	Updated elevation tracking rate
BAZOUT	Actual boresight azimuth angle

Inputs and outputs for the major routines implementing Angle Track FE are given in Tables 2.27-3 through 2.27-7. All inputs and outputs are dedicated to the Angle Track FE.

TABLE 2.27-3. Subroutine RESLV2 Inputs and Outputs.

SUBROUTINE: RESLV2					
Inputs			Outputs		
Name	Type	Description	Name	Type	Description
IRADFL	Argument	Radar type flag 1=ACQ, 2=TRACK, 3=SEEK, 4=ILLUM	REFCHI	Argument	In-phase reference signal
NUMPRO	Argument	Number of signals generated by the antenna response modules	REFCHQ	Argument	Quadrature reference signal
TIMEG	Argument	Simulation time	SGDVA	Argument	Azimuth channel difference voltages

TABLE 2.27-3. Subroutine RESLV2 Inputs and Outputs. (Contd.)

SUBROUTINE: RESLV2					
Inputs			Outputs		
Name	Type	Description	Name	Type	Description
RESCF	Common DMOD2C	Resolver frequency	SGDVE	Argument	Elevation channel difference voltages
SGDVA	Argument	Azimuth channel difference voltages			
SGDVE	Argument	Elevation channel difference voltages			
SGSV	Argument	Sum channel voltages			

TABLE 2.27-4. Subroutine DEMOD2 Inputs and Outputs.

SUBROUTINE: DEMOD2					
Inputs			Outputs		
Name	Type	Description	Name	Type	Description
DT	Input Argument	Time between samples	AZERR	Argument	Azimuth off- boresight error angle
ERCNAZ	Argument	Azimuth antenna error slope	ELERR	Argument	Elevation off- boresight error angle
ERCNEL	Argument	Elevation antenna error slope	ICOUNT	Common DMOD2C	Inner product stack index
FCTVIS	Argument	Fraction of signal pulse visible in the range gate	NLATCH	Common DMOD2C	Stack - full flag 1 = full 0 = not full
IRADFL	Argument	Radar type flag 1=ACQ, 2=TRACK 3=SEEK, 4=ILLUM	SINPAZ	Common DMOD2C	Azimuth error channel working inner product
NUMPRO	Argument	Number of signals generated by the antenna response modules	SINPEL	Common DMOD2C	Elevation error channel working inner product
REFCHI	Argument	In-phase reference signal			
REFCHQ	Argument	Quadrature reference signal			
SGDVA	Argument	Azimuth difference signal voltages			
SGDVE	Argument	Elevation difference signal voltages			
MRADFL	Common ARYBND	Array bound Parameter = 4			
ICOUNT	Common DMOD2C	Inner product stack index			
NLATCH	Common DMOD2C	Stack-full flag 1=full 0=not full			
NRSAMPL	Common DMOD2C	Number of samples in the demodulator stack			
RESCF	Common DMOD2C	Resolver frequency			
SINPAZ	Common DMOD2DC	Azimuth error channel working inner product			
SINPEL	Common DMOD2C	Elevation error channel working inner product			

TABLE 2.27-5. Subroutine ANTPOI Inputs and Outputs.

SUBROUTINE: ANTPOI					
Inputs			Outputs		
Name	Type	Description	Name	Type	Description
RSKSRV	Common ANTSVO	Locke's open-loop gain constant	AZRAT1	Argument	Azimuth rate difference equation output one time step back
RSNSRV	Common ANTSVO	Locke's parameter for open-loop transfer functions	ELRAT1	Argument	Elevation rate difference equation output one time step back
TLPANT	Common ANTSVO	Servo time-step	AZRATE	Argument	Azimuth rate difference equation output
W1	Common ANTSVO	Locke's parameter W1	ELRATE	Argument	Elevation rate difference equation output
IDTIN	Common FLAGS	Time-step changed flags	AZSVI1	Argument	Azimuth difference equation input one time step back
IRADFL	Common FLAGS	Radar type flag 1=ACQ, 2=TRACK 3=SEEK, 4=ILLUM	ELSVI1	Argument	Elevation difference equation input one time step back
KFIRST	Common FLAGS	First time through subroutine flag	AZVIN	Argument	Azimuth difference equation input
BOREAZ	Common FREND	Boresight azimuth angle	ELVIN	Argument	Elevation difference equation input
GDT	Common GRADAR	System time-step	IRNSLP	Argument	Number of servo increments in a system time step
BOREEL	Common FREND	Boresight elevation angle	RSCA1	Argument	Difference equation coefficient
DTMAX	Common SVOVAR	Maximum time interval allowed	RSCA2	Argument	Difference equation coefficient
			RSCA3	Argument	Difference equation coefficient
			RSCA4	Argument	Difference equation coefficient
			RSCA5	Argument	Difference equation coefficient
			RSCA6	Argument	Difference equation coefficient
			RSCA7	Argument	Difference equation coefficient
			TLPANT	Common ANTSVO	Servo time step

TABLE 2.27-6. Subroutine SVOEXC Inputs and Outputs.

SUBROUTINE: SVOEXC					
Inputs			Outputs		
Name	Type	Description	Name	Type	Description
IDTIN	Common FLAGS	Time-step changed flag	BAZOUT	Common FRIEND	Measured Azimuth angle
IRADFL	Common FLAGS	Radar type flag 1=ACQ, 2=TRACK 3=SEEK, 4=ILUM	AZRATE	Common RATES	Azimuth antenna rate
KFIRST	Common FLAGS	First time through subroutine flag	ELRATE	Common RATES	Elevation antenna rate
BOREAZ	Common FRIEND	Boresight Azimuth angle	BOREAZ	Common FRIEND	Boresight Azimuth angle
BOREEL	Common FRIEND	Boresight Elevation angle	BOREEL	Common FRIEND	Boresight Elevation angle
AZMZAN	Common GRADAR	Measured Azimuth error angle			
ELMZAN	Common GRADAR	Measured Elevation error angle			
AZRATE	Common RATES	Azimuth antenna motion rate			
ELRATE	Common RATES	Elevation antenna motion rate			

Table 2.27-7 below summarizes the input and output variables for subroutine SUMDIF.

TABLE 2.27-7. Subroutine SUMDIF Inputs and Outputs.

SUBROUTINE: SUMDIF					
Inputs			Outputs		
Name	Type	Description	Name	Type	Description
FCTVIS	Argument	Fraction of the signal pulse visible in the range gate	SAZERR	Argument	Azimuth off-boresight error angles
NUMPRS	Argument	Number of signals generated by the antenna response modules	SELERR	Argument	Elevation off- boresight error angles
SAZSLP	Argument	Azimuth antenna error slope			
SELSLP	Argument	Elevation antenna error slope			
SKSDFA	Argument	Azimuth difference channel signal			
SKSDFE	Argument	Elevation difference channel signal			
SKSGSV	Argument	Sum channel difference signals			
EPSILN	Common CONST	A very small number			
PI2	Common CONST	2			

2.27.4 Assumptions and Limitations

Two approaches are taken to implement the antenna positioning servo. A generic approach that simplifies certain dynamic elements and a system specific approach that retains the detail of the individual dynamic elements. Due to this detail, the system specific code is normally classified as SECRET/NOFORN/WNINTEL. The generic approach is so named because it can be implemented as unclassified code.

The full servo configuration is represented by the feedback diagram shown in Figure 2.27-3. In the generic approach, the inner loop involving the positioning motor and tachometer dynamics is assumed to achieve a steady-state response much sooner than the outer loop. Hence the inner loop can be collapsed to a constant gain and the entire system can be represented as a single feedback loop. It has been demonstrated that reasonably good results can be obtained for some systems using this generic representation.

The system specific servo code maintains a higher level of detail, and is therefore more representative of certain systems. The important implementation results however involve the derivation of the servo difference equations by root-matching methods. This method is discussed in Design Element 27-5.

